# Detector-to-detector Compton backscattering in germanium at 59.5 keV

**Pašić, Selim; Ilakovac, Ksenofont**

*Source / Izvornik:* **Physical Review A, 1997, 55, 4248 - 4252**

**Journal article, Published version**
**Rad u časopisu, Objavljena verzija rada (izdavačev PDF)**

https://doi.org/10.1103/PhysRevA.55.4248

*Permanent link / Trajna poveznica:* https://urn.nsk.hr/urn:nbn:hr:217:893799

*Rights / Prava:* In copyright / Zaštićeno autorskim pravom.

*Download date / Datum preuzimanja:* **2024-05-13**

*Repository / Repozitorij:*

Repository of the Faculty of Science - University of Zagreb

# Detector-to-detector Compton backscattering in germanium at 59.5 keV

S. Pašić
*Department of Physics, Faculty of Science, University of Zagreb, Bijenička cesta 32, HR-10000 Zagreb, Croatia*

K. Ilakovac
*Department of Physics, Faculty of Science, University of Zagreb, Bijenička cesta 32, HR-10000 Zagreb, Croatia and R. Bošković Institute, P.O. Box 1016, 10001 Zagreb, Croatia*

(Received 15 October 1996; revised manuscript received 19 February 1997)

The differential cross section for Compton scattering $d^2\sigma/d\Omega dE$ in germanium ($Z=32$) was measured using the sensitive volume of a Ge detector as the scatterer and another Ge detector for detection of the scattered radiation, at an incident energy of 59.537 keV and a scattering angle of about 170°. The application of the coincidence technique and the requirement of a constant energy sum yield a clear spectrum in a broad energy range. Detailed analyses of the processes involved in the detector-to-detector scattering were made, including various double-scattering processes. Calculations show that bremsstrahlung of photoelectrons dominates at low energies, while all double-scattering processes weakly contribute to the coincidence rates. The influence of Compton-Rayleigh and Rayleigh-Compton scattering on Compton data is relatively stronger at high energy, while an approximate proportionality of Compton-Compton and single Compton spectra at scattering angles close to 180° was obtained, assuming the impulse approximation. Single and double Compton scattering on stationary electrons at 180° have been shown to produce photons of exactly the same energy. The measured differential cross sections for Compton scattering and results of calculations based on the impulse approximation are in fair agreement. [S1050-2947(97)06306-3]

PACS number(s): 32.80.Cy, 32.30.Rj

## I. INTRODUCTION

Compton scattering is an important collision process of x and $\gamma$ rays in matter. Therefore, the interest for developing theoretical [1] and experimental techniques with the aim to determine accurately Compton scattering still persists [2]. Almost all prior measurements of the differential Compton-scattering cross section $d^2\sigma/d\Omega dE$ on bound atomic electrons have been obtained using the singles-mode measurements, i.e., the source-scatterer-detector assembly [3,4]. However, in this type of measurement, partial energy absorption in the detector, of photons scattered by Compton effect on weakly bound electrons, leads to a strong increase of the counting rate below the Compton peak [3,4]. Therefore, at photon energies below the Compton peak, where the differential cross section drops to less than about 2% of the values in the peak, the singles mode does not give reliable results.

In our previous work [5] we presented another approach for measuring Compton cross section for germanium atom using two germanium detectors in coincidence. The sensitive volume of one of the detectors was used as the target and detector of recoil electrons and the other detector was used as the detector of scattered radiation. Coincidences of pulses from the two detectors were recorded. If there is no energy loss, coincidence events satisfy the condition $E_1+E_2=E_0$, which is equal to the energy of the incident photon. Only events in the ''events line'' $E_1+E_2=E_0$ in the $E_1$-$E_2$ plane were analyzed. A clear spectrum in a broad energy range was obtained. We noted several important advantages of the coincidence method of measurement [5]. (a) Background due to exterior radiation is negligible because of the requirement of simultaneity of pulses from the two detectors. (b) The coincidence method allows one to distinguish Compton events from some other events (e.g., from events due to elastic scattering). (c) Partial absorption of energy of either the recoil electron in the detector-scatterer or the Compton scattered photon in the second detector does not appear as an event on the $E_1+E_2=E_0$ events line. Hence the problem of deconvolution because of the detector response is eliminated.

In this work we present measurements of Compton backscattering in germanium at an incident energy of 59.54 keV, made with an improved experimental arrangement. Only one detector served as the scatterer (the ''first'' detector) and another served as detector of scattered radiation (the ''second'' detector). This arrangement allowed the study of the detector-to-detector scattering at considerably lower energies of scattered radiation. The processes involved in detector-to-detector scattering are important in processing the Compton data. Therefore, detailed calculations of these processes and analyses of their influence on Compton spectrum have been made.

To the authors' knowledge, no measurement of the Compton spectrum due to scattering by bound electrons using the coincidence method with a pair of semiconductor detectors has been published by other authors so far. A similar experimental procedure for measuring $d^2\sigma/d\Omega dE$ on $K$ electrons of germanium, using three detectors, was reported [6,7]. The coincidence technique with two scintillation detectors was used in measurements of the angular distribution of the Compton scattered $\gamma$ rays [8]. The coincidence technique was also applied to test simultaneity in the Compton effect (see Ref. [9] and references therein).

## II. APPARATUS

In the present arrangement (see Fig. 1), a small ''central'' shield was used to absorb $\gamma$ rays emitted towards the second

 © 1997 The American Physical Society

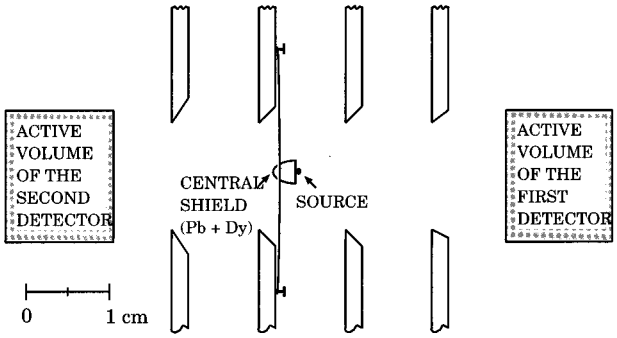


FIG. 1. Experimental arrangement used in the Compton scattering measurement.

detector. The central shield was made of lead of an approximately semispherical shape and a thickness of about 0.7 mm. The cavity (about 1 mm in diameter) was filled with $Dy_2O_3$ and was covered by a thin disk of Plexiglas.

Tiny chips of $^{241}$Am were embedded in a small (about 0.2 mm in diameter) ball of glue. The activity of the source was 39 kBq, as determined by a comparison with a calibrated source of $^{241}$Am. The source was centered on the Plexiglas disk of the central shield and was mounted in the center of a 15-mm-diam hole in one of four 2-mm-thick lead plates that were placed between the detectors. The lead plates defined the scattering angle at about $\vartheta_p \approx 170°$ with an angular divergence of $-2°$ to $+5°$. These plates also reduced scattering from the cylindrical lead shield that surrounded the experimental setup shown in Fig. 1.

Two planar high-purity germanium detectors (supplied by ORTEC), nominally 200 mm$^2 \times 13$ mm thick, were used in the measurements. Pulses from the detectors were fed into a fast-slow coincidence system with a three-parameter $128 \times 512 \times 512$ channel pulse-height analyzer. For each event, the time difference and the energy in each detector were recorded. Coincidence unit was set to $2\tau = 200$ ns. The full width at half maximum time resolution was about 20 ns. The energy resolution of the detectors at an energy of 59.537 keV was about 360 eV. The time duration of the measurements was 549 h.

## III. ANALYSIS OF DETECTOR-TO-DETECTOR SCATTERING

The data in the events line $E_1 + E_2 = E_0$ in the $E_1$-$E_2$ spectrum were analyzed. The spectrum obtained is shown in Fig. 2 without correction. It contains not only the events due to single Compton (SC) scattering, but also events from other processes. Most important are the following: (a) crosstalk among the two detectors via characteristic Ge x rays; (b) bremsstrahlung of electrons ejected by photoeffect of incident photons; (c) single Compton scattering in the second detector due to imperfect asymmetry of the experimental setup (a negligible contribution to the recorded data); and (d) double Rayleigh-Compton (RC), Compton-Rayleigh (CR), and Compton-Compton (CC) scattering. The processes were classified into single [SC and (a)–(c)] and double [(d)] scattering processes.

We calculated the numbers of events for each type of scattering. Calculations were performed on an absolute scale

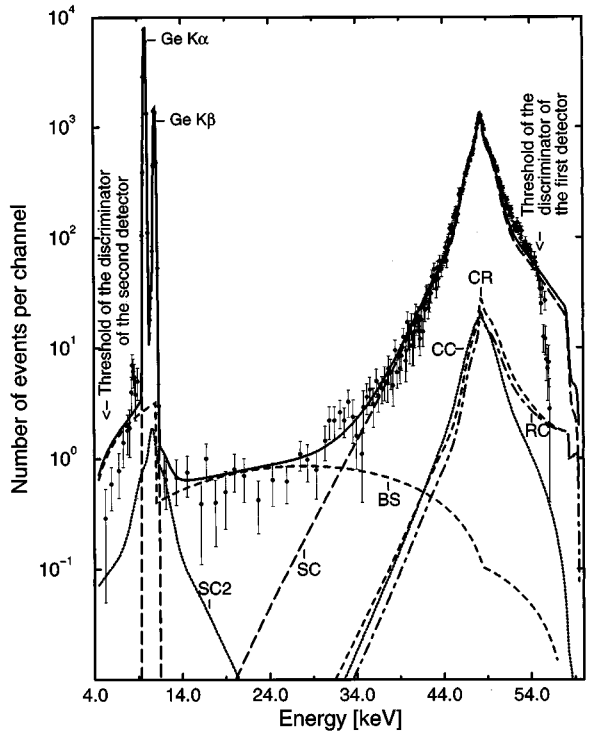


FIG. 2. Experimental data and calculated numbers of events of processes involved in detector-to-detector scattering. The curves show the following: SC, single Compton scattering in the target; BS, bremsstrahlung of photoelectrons ejected by incident radiation; Ge $K\alpha$ and Ge $K\beta$, peaks due to characteristic x rays of germanium; SC2, single Compton scattering in the second detector; CC, RC, and CR, Compton-Compton, Rayleigh-Compton, and Compton-Rayleigh double scattering.

except for process (a), from which the solid angle was determined. Single and multiple numerical integration procedures with an accuracy greater than $10^{-4}$ were used. The results of the calculations are shown in Fig. 2.

In order to considerably simplify the calculation of the numbers of events due to double scattering, normal incidence, infinite thickness, and infinite radius of the cylindrical target (the first detector) were assumed. For the purpose of comparison, the same assumptions were also taken in deriving the expression for single scattering. From the geometry of the setup and while $1/\mu(E_0) \ll D$ is the thickness of the target, the first two assumptions have a small or negligible influence on the calculated results. The infinite radius of the cylindric target, which could strongly influence calculated double-scattering results, is a very good approximation in our experiment since $\mu R_f \geqslant 10$, where $R_f$ is radius of the target [10]. Also, in deriving the expression (3) for the numbers of events for double scattering (see below), polarization effects were neglected. For details of their possible influence on double-scattering processes see Ref. [11].

### A. Single scattering

The theoretical numbers of events due to single-scattering processes were calculated using the relation

$$n(E) = N_0 \frac{d^2\sigma/d\Omega dE}{\mu(E_0) + \mu(E)/\cos(170°)} \Delta D, \qquad (1)$$

where $n(E)$ is the number of events per channel, $N_0$ is the number of photons of incident energy $E_0$ recorded by the first detector, $d^2\sigma/d\Omega dE$ is the differential cross section, and $\mu(E_0)$ and $\mu(E)$ are the attenuation coefficients in germanium [12,13] for the incident energy and energy $E$ of scattered photon.

$$\Delta D = \epsilon_c \epsilon_2 \epsilon(E) N_{\mathrm{Ge}} A_2 \exp[-\mu_{\mathrm{air}}(E) d] \Delta\Omega,$$

where $\epsilon_c = 0.97$ is the efficiency of the coincidence, $\epsilon_2 = 0.95$ is the estimated efficiency (not including the escape of characteristic Ge x rays) of the second detector, $\epsilon(E)$ gives the efficiency of the second detector involving only the escape of characteristic Ge x rays, $N_{\mathrm{Ge}}$ is atomic density in germanium, $A_2 = 0.12$ keV/channel is the channel width, $\mu_{\mathrm{air}}$ is the attenuation coefficient in air, $d$ is an average path length of scattered photons in air, and $\Delta\Omega = 0.104$ sr is the average solid angle of the second detector as viewed from the collision point in the first detector.

When calculating the Compton spectrum using Eq. (1), the impulse approximation [14,15] for the whole germanium atom was used. The results obtained were convoluted with a Gaussian function representing the detector response function (not including escape processes). If we take into account the incident energy and the binding energies of target electrons, the conditions for the application of the impulse approximation are justified [14,16].

The bremsstrahlung of electrons ejected by photoeffect caused by incident photons was calculated using the expression

$$\left(\frac{d^2\sigma}{d\Omega dE}\right)_{\mathrm{bs}} = \frac{\sigma_K}{4\pi}\frac{1}{E}\int_E^{E_0-E_K} \frac{\frac{d}{dE}\left(\frac{dT}{ds}\right)_{\mathrm{rad},E}}{\left(\frac{dT}{ds}\right)_{\mathrm{rad}} + \left(\frac{dT}{ds}\right)_{\mathrm{ion}}} dE + \frac{\sigma_L}{4\pi}\frac{1}{E}\int_E^{E_0-E_L} \frac{\frac{d}{dE}\left(\frac{dT}{ds}\right)_{\mathrm{rad},E}}{\left(\frac{dT}{ds}\right)_{\mathrm{rad}} + \left(\frac{dT}{ds}\right)_{\mathrm{ion}}} dE, \quad (2)$$

where $\sigma_K$ and $\sigma_L$ are total cross sections for photoelectric absorption by the $K$ and $L$ electrons of germanium [12], respectively, and $E_K$ and $E_L$ are the binding energies of the $K$ or $L$ electrons. The integrals represent the probabilities of production of the bremsstrahlung photon per electron of an initial kinetic energy $E_0 - E_K$ or $E_0 - E_L$ and per energy interval $dE$. $(dT/ds)_{\mathrm{rad}}$ and $(dT/ds)_{\mathrm{ion}}$ are expressions for energy loss per unit path length to radiation and ionization, respectively, of an electron of kinetic energy $T$ [17,18], and from them $(d/dE)(dT/ds)_{\mathrm{rad}}$ was derived according to Ref. [19].

### B. Double scattering

The expression for the numbers of events per channel for double scattering, obtained in the limit of infinite thickness of the target, is given by [20]

$$n(E) = 2N_0 \Delta D \int dE_1 \int_0^{\pi} d\varphi \left( \int_0^1 SF_1 dx_1 + \int_{-1}^0 SF_2 dx_1 \right), \quad (3)$$

where

$$S = N_{\mathrm{Ge}} \frac{d^2\sigma_1(E_0, E1, x_1)}{d\Omega_1 dE_1} \frac{d^2\sigma_2(E_1, E, x_2)}{d\Omega_2 dE},$$

$$F_1 = \frac{1}{\mu(E_0) - \mu(E)/x_p} \frac{1}{\mu(E_1) - \mu(E)x_1/x_p},$$

and

$$F_2 = \left( \frac{1}{\mu(E_0) - \mu(E)/x_p} - \frac{1}{\mu(E_0) - \mu(E_1)/x_1} \right) \frac{1}{\mu(E_1) - \mu(E)x_1/x_p}.$$

$E_1$ and $E$ are energies after the first and second scattering, respectively, $x_1 = \cos\vartheta_1$, $x_2 = \cos\vartheta_2$, and $x_p = \cos\vartheta_p$, where $\vartheta_1$ and $\vartheta_2$ are angles of the first and second scattering respectively, and $\vartheta_p = 170°$ is the average angle between the incident and double-scattered photon. From the geometry of double scattering follows [20]

$$x_2 = \sqrt{1 - x_p^2}\sqrt{1 - x_1^2} \cos\varphi + x_p x_1. \quad (4)$$

In calculating the double-scattering processes, the impulse approximation was also used for the Compton cross section for the whole germanium atom. The differential cross section for Rayleigh (elastic) scattering was derived from Ref. [21], where a relativistic Hartree-Fock-Slater modified atomic form factor was tabulated. The calculations of the elastic-scattering cross sections have also been made using the values of the form factor from Ref. [22], and very nearly equal results were obtained for the momentum transfers of interest in the present experiment.

### C. Influence of double-scattering processes on Compton spectrum

Integration in the photon energy range from 25 keV up to 59.5 keV of single-Compton and all double-scattering cross sections shows that the ratio $Q$ of all double-scattering events to the total of Compton-single-scattering events is 2.3% for RC, 2.9% for CR, and 2.1% for CC scattering. These numbers do not tell us much about the contribution of double-scattering data to single-Compton-scattering data because the shapes of the spectra are different. RC and CR spectra have a very similar shapes, but differ from the single-scattering Compton spectrum. Their influence on the Compton data is relatively stronger in the high-energy region and weaker for other energies. Calculations show that RC and CR scattering data reach Compton data at the upper-energy end of the spectrum for incident energies greater than 60 keV. On the other hand, the spectrum of CC scattering is approximately proportional to the single-scattering Compton spectrum at backscattering angles close to 180°. That is a surprising result. In the following we show that in the case of stationary electrons and observing at scattering angle of

TABLE I. Ratios of Compton-Compton to single Compton scattering at angles $170° \leq \vartheta_p \leq 180°$ over a broad energy range, when conditions for the application of the impulse approximation are fulfilled.

| $E_0$ (keV) | $Q$ (%) |
|---|---|
| 30 | 0.30 |
| 40 | 0.70 |
| 50 | 1.33 |
| 59.54 | 2.14 |
| 80 | 4.62 |

$\vartheta_p = 180°$, both processes yield photons of the same single-valued energy. In double scattering, energies of photons after the first and second Compton scattering are

$$E_1 = \frac{E_0}{1+E_0(1-x_1)}, \quad E = \frac{E_1}{1+E_1(1-x_2)}, \tag{5}$$

where $x_1$ and $x_2$ are cosines of the two scattering angles. Eliminating $E_1$ gives the energy of the double-Compton-scattered photon:

$$E = \frac{E_0}{1+E_0(2-x_1-x_2)}. \tag{6}$$

For double scattering at $\vartheta_p = 180°$, the sum of the two scattering angles also equals 180°. So $x_1 = -x_2$ and

$$E = \frac{E_0}{1+2E_0},$$

which is also the photon energy after single Compton scattering at the scattering angle of 180°. That result could have been inferred by extrapolating the calculated single- and double-Compton-scattered photon energies for 0°–150° scattering angles in Table I of Ref. [23] to 180°.

The initial momenta of the electrons broaden the two spectra. Numerical calculations of single and double Compton spectra using the impulse approximation for incident energies from 20 keV to 80 keV have shown that broadening of spectra is similar. That causes an approximately uniform contribution of the double-Compton-scattering events to the single Compton spectrum. That relation can be applied to estimate the double Compton spectrum (e.g., in a two-photon transition experiment [24]). The CC spectrum can be estimated using the single Compton spectrum and percentages from Table I.

### D. Experimental differential cross section for Compton scattering

The experimental differential cross section $d^2\sigma/d\Omega dE$ for Compton scattering is shown in Fig. 3 on an absolute scale together with the theoretical calculation based on the impulse approximation. The indicated standard deviations of the data are statistical only. An uncertainty of the absolute values of double-differential Compton cross sections due to the geometrical factors (not shown in Fig. 3) is about 4%. In deriving the experimental cross sections, the calculated numbers of events due to double scattering (RC, CR, and CC)

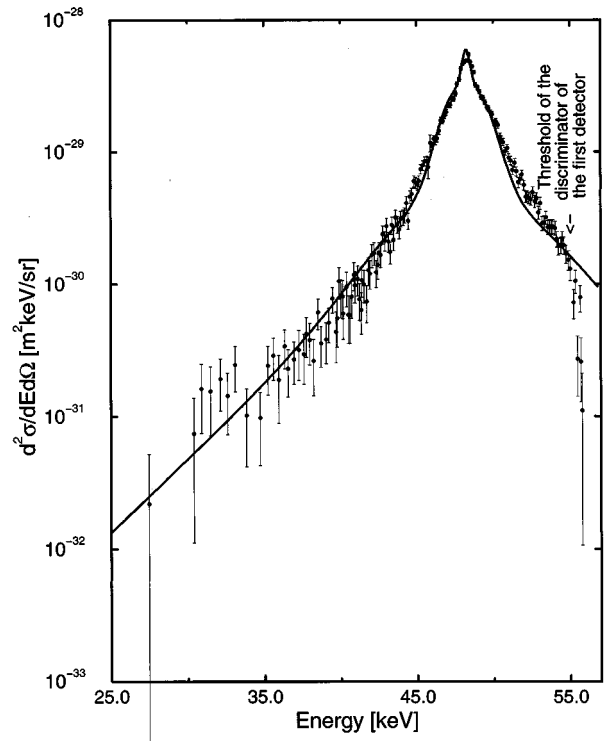


FIG. 3. Experimental differential cross section for Compton scattering and results of calculations using the impulse approximation.

and bremsstrahlung were subtracted from the original data and the new spectrum was subsequently converted into the differential cross section using the relation

$$\left(\frac{d^2\sigma}{d\Omega dE}\right)_{\text{expt}} = \frac{n_{\text{expt}}[\mu(E_0)+\mu(E)/\cos(170°)]}{N_0 \Delta D}. \tag{7}$$

The presented energy range from 25 keV to 55 keV is about half of the whole energy range. It is limited by bremsstrahlung data at the low energies and by the threshold of the discriminator of the first detector ($\simeq$ 5 keV) at the upper-energy end. The transition from bremsstrahlung to Compton data is sharp and only a few low-energy points in Fig. 3 are strongly affected by bremsstrahlung. All other data are essentially pure single-Compton-scattering data.

The integration of the experimental differential cross sections over photon energy gives the value of the incoherent scattering function $S_{\text{expt}}(4.8,32) = 31.1 \pm 0.2$. It is in good agreement with the tabulated value $S(4.8,32) = 30.78$ obtained from Ref. [22].

## IV. SUMMARY

The coincidence method is a very good experimental technique for measuring the spectrum due to Compton scattering in germanium atoms. The energy range is evidently considerably wider than what may be expected from the singles-mode measurement of Compton scattering in germanium. The Compton spectrum obtained is clear and there is no need for numerous corrections. Thus the possibility of systematic errors in the final results is largely reduced. Only corrections for bremsstrahlung of photoelectrons at the low-

energy end and possibly for Rayleigh-Compton and Compton-Rayleigh scattering at the upper-energy end of the spectrum were needed. Compton-Compton scattering approximately uniformly affected Compton-backscattered data. A simple calculation shows that single and double Compton backscattering ($\vartheta_p = 180°$) on stationary electrons gives scattered photons of exactly the same energy. The results of numerical calculations based on the impulse approximation have shown that broadening of spectra of the single- and double-backscattered photons due to motion of electrons are similar.

Considering the absolute scale of the experimental differential cross sections $d^2\sigma/d\Omega dE$ for Compton scattering in germanium for 59.537 keV photons at the scattering angle of 170°, good agreement with the theoretical values based on the impulse approximation has been found in most of the measured energy range, but in some parts deviations have been found. Also, good agreement between the experimental value of the incoherent scattering function and the corresponding tabulated value in Ref. [22] has been obtained.

## ACKNOWLEDGMENTS

We wish to thank Dr. T. Surić for helpful discussions of the theory of Compton scattering. We express our sincere thanks to Dr. D. E. Cullen of Lawrence Livermore National Laboratory and to Dr. J. H. Hubbell of National Institute of Standards and Technology for sending us recent tables for the x-ray attenuation coefficients, total cross sections, and other data.

[1] T. Surić, P. M. Bergstrom, Jr., K. Pisk, and R. H. Pratt, Phys. Rev. Lett. **67**, 189 (1991).
[2] P. P. Kane, Phys. Rep. **218**, 67 (1992).
[3] P. Rullhusen and M. Schumacher, J. Phys. B **9**, 2435 (1976).
[4] M. Schumacher, Z. Phys. **242**, 444 (1971).
[5] S. Pašić and K. Ilakovac, Fizika B **4**, 127 (1995).
[6] M. Pradoux, H. Meunier, J. Bauman, and G. Roche, Nucl. Instrum. Methods **112**, 443 (1973).
[7] M. Pradoux, H. Meunier, M. Avan, and G. Roche, Phys. Rev. A **16**, 2022 (1977).
[8] R. Hofstadter and J. A. McIntyre, Phys. Rev. A **76**, 1269 (1949).
[9] Z. Bay, V. P. Henri, and F. McLernon, Phys. Rev. A **97**, 1710 (1955).
[10] A. C. Tanner and I. Epstein, Phys. Rev. A **14**, 328 (1976).
[11] J. E. Fernández, J. H. Hubbell, A. L. Hanson, and L. V. Spencer, Radiat. Phys. Chem. **41**, 579 (1993).
[12] D. E. Cullen *et al.*, Lawrence Radiation Livermore Laboratory, Report No. UCRL-ID-103424, 1990 (unpublished); D.E. Cullen *et al.*, Lawrence Livermore National Laboratory, Report No. UCRL-50400, Vol. 6, Rev. 4, 1989 (unpublished).
[13] J. H. Hubbell and S. M. Seltzer, National Institute of Standards and Technology Report No. NISTIR 5632, 1995 (unpublished).
[14] P. Eisenberger and P. M. Platzman, Phys. Rev. A **2**, 415 (1970).
[15] M. Schumacher, F. Smend, and I. Borchert, J. Phys. B **8**, 1428 (1975).
[16] T. Surić, Nucl. Instrum. Methods Phys. Res. Sect. A **314**, 240 (1992).
[17] R. D. Evans, *The Atomic Nucleus* (McGraw-Hill, New York, 1955).
[18] W. Heitler, *Quantum Theory of Radiation*, 3rd ed. (Oxford University Press, London, 1954).
[19] K. Ilakovac, J. Tudorić-Ghemo, V. Horvat, N. Ilakovac, S. Kaučić, and M. Vesković, Nucl. Instrum. Methods Phys. Res. Sect. A **245** 467 (1986).
[20] A. C. Tanner and I. Epstein, Phys. Rev. A **14**, 313 (1976).
[21] D. Schaupp, M. Schumacher, F. Smend, P. Rullhusen, and J. H. Hubbell, J. Phys. Chem. Ref. Data **12**, 467 (1983).
[22] J. H. Hubbell, Wm. J. Veigele, E. A. Briggs, R. T. Brown, D. T. Cromer, and R. J. Howerton, J. Phys. Chem. Ref. Data **4**, 471 (1975).
[23] E. Hayward and J. H. Hubbell, J. Appl. Phys. **25**, 506 (1954).
[24] K. Ilakovac, V. Horvat, Z. Krečak, G. Jerbić-Zorc, N. Ilakovac, and T. Bokulić, Phys. Rev. A **46**, 132 (1992).